

Transcript Profiles of *Candida albicans* Cortical Actin Patch Mutants Reflect Their Cellular Defects: Contribution of the Hog1p and Mkc1p Signaling Pathways†

Ursula Oberholzer,¹ André Nantel,¹ Judith Berman,² and Malcolm Whiteway^{1*}

Biotechnology Research Institute, National Research Council of Canada, 6100 Royalmount, Montreal H4P 2R2, Quebec, Canada,¹ and Department of Genetics, Cell Biology & Development, University of Minnesota, 6-160 Jackson Hall, 321 Church St. SE, Minneapolis, Minnesota 55455²

Received 23 December 2005/Accepted 14 June 2006

In *Candida albicans*, Myo5p and Sla2p are required for the polarized localization and function of cortical actin patches, for hyphal formation, and for endocytosis. Deletion of either the *MYO5* or the *SLA2* gene generated a common transcriptional response that involved changes in the transcript levels of cell wall protein- and membrane protein-encoding genes. However, these profiles were distinct from those observed for a mutant with specific deletions of the actin-organizing domains of Myo5p or for wild-type cells treated with cytochalasin A, both of which also generate defects in the organization of cortical actin patches. The profiles observed for the *myo5Δ* and *sla2Δ* mutants had similarities to those of wild-type cells subjected to an osmotic shock, and the defects in cortical patch function found with *myo5Δ* and *sla2Δ* mutants, but not cortical actin patch distribution per se, affected sensitivity to various stresses, including heat and osmotic shocks and cell wall damage. Secondary effects coupled with defective endocytosis, such as lack of polarized lipid rafts and associated protein Rvs167-GFP (where GFP is green fluorescent protein) and lack of polarized wall remodeling protein GFP-Gsc1, were also observed for the *myo5Δ* and *sla2Δ* mutants. The mitogen-activated protein kinases Hog1p and Mkc1p, which mediate signaling in response to osmotic stress and cell wall damage, do not play a major role in regulating the transcript level changes in the *myo5Δ* and *sla2Δ* mutants. Hog1p was not hyperphosphorylated in the *myo5Δ* and *sla2Δ* mutants, and the transcript levels of only a subset of genes affected in the *myo5Δ* mutant were dependent upon the presence of Hog1p and Mkc1p. However, it appears that Hog1p and Mkc1p play important roles in the *myo5Δ* mutant cells because double deletion of myosin I and either Hog1p or Mkc1p resulted in very-slow-growing cells.

Organisms are capable of responding to a variety of environmental stresses. In the budding yeast *Saccharomyces cerevisiae* and the related pathogenic yeast *Candida albicans*, activation of the stress response pathways involves mechanisms for sensing a particular stress and conveying the signal via mitogen-activated protein kinase (MAPK) modules to key effectors. Effectors include transcription factors that regulate the expression of specific genes in response to stress. The proteins encoded by these genes help cells repair the damage inflicted and generally increase resistance to stress (43, 48, 49). Stresses include rapid changes in external osmolarity and temperature and insults to the cell wall, to DNA, and to the actin cytoskeleton. Some stresses have pleiotropic effects; for example, hyper- and hypoosmotic stresses cause not only ion imbalance and cell shrinkage or swelling but also a rapid although transient depolarization of the actin cytoskeleton (7, 23, 26, 60). Perturbations of the actin cytoskeleton are known to arrest dividing cells until the damage is repaired (25). Repolarization of the actin cytoskeleton appears to be a critical step in the recovery response and required for cells to resume cellular division.

Mechanisms that trigger repolarization of the actin cytoskeleton are poorly understood but may involve the very same signaling components involved in responding to stress in the first place. For example, repolarization of the actin cytoskeleton following a hypoosmotic shock involves the cell wall sensors Wcs1p and Mid2p, which are both potential activators of the Pkc1p-Slt2p cell wall integrity pathway (23). Repolarization of the actin cytoskeleton following a hyperosmotic shock requires the activity and proper polarized localization of the MEKKK Ssk2p of the Sln1p branch of the Hog1-dependent pathway (60). It is postulated that Ssk2p may control the activity of Bni1p and other proteins of the actin cytoskeleton to promote actin repolarization. Rvs161p, organizer of the actin cytoskeleton and component of lipid rafts, has also been shown to play a role in the repolarization of actin following a hyperosmotic shock (7). Finally, Ras2p is necessary for actin repolarization following a mild heat shock (26).

The actin cytoskeleton of the fungal pathogen *C. albicans* plays a key role in morphogenesis and hyphal formation (1, 4, 5, 32, 41, 55, 58). In yeasts, this cytoskeleton is comprised of cortical actin patches found at sites of polarized growth and actin cables that serve as tracks for secretion of vesicles to sites of polarized growth (11, 45, 46). Components of the cortical actin patches are also required for endocytosis in *S. cerevisiae* (15, 45). Indeed, cortical actin patches are the actual sites of endocytosis (29). *S. cerevisiae* myosin I (Myo3/5p) and Sla2p have been shown to play important roles in organizing the

* Corresponding author. Mailing address: Biotechnology Research Institute, National Research Council of Canada, 6100 Royalmount, Montreal H4P 2R2, Quebec, Canada. Phone: (514) 496-6146. Fax: (514) 496-6213. E-mail: malcolm.whiteway@nrc-cnrc.gc.ca.

† Supplemental material for this article may be found at <http://ec.asm.org/>.

actin cytoskeleton and mediating endocytosis by the cortical actin patches (18, 28, 33, 34). In addition, *C. albicans* *SLA2* and *MYO5* are required for hyphal formation, *MYO5* being the unique gene encoding myosin I, hereby designated Myo5p (5, 41).

The *C. albicans* *sla2Δ* and *myo5Δ* mutants suffer similar related complications, including a disorganized actin cytoskeleton and endocytic defects. These defects may trigger cellular responses, such as constitutive activation of the Hog1p and Pkc1p-Slt2p stress response pathways, to compensate for permanent cortical actin patch depolarization and malfunction. Understanding the extent of these defects will shed light on the physiological role of Sla2p and Myo5p and may reveal how wild-type cells normally respond to direct perturbations of the actin cytoskeleton. In the present study, we have used genome-wide transcript profiling as a tool for analyzing complex phenotypes, with a goal of understanding the physiological roles of *C. albicans* Myo5p and Sla2p during vegetative and hyphal growth. We have found that mutations in these proteins affect endocytic-related functions in membrane and cell wall biogenesis and play an important role in tolerance to stress. Unexpectedly, these defects are reflected in the transcript profiles obtained, validating the use of this genome-wide approach in uncovering the physiological roles of cellular components. However, neither the Hog1p nor the Pkc1p-Slt2p pathway appears to be hyperactivated in these mutants, suggesting that these pathways do not play a central role in response to permanent perturbations of the actin cytoskeleton in *C. albicans*.

MATERIALS AND METHODS

DNA manipulations. The *RVS167-GFP* construct was made by PCR amplification using primers UO87 and UO114 and genomic DNA as a template. The 2.6-kb PCR product was cloned into pVEC as a BamHI-XbaI fragment (pU158). The XhoI and NsiI restriction sites were added 3' to the BAR sequence at nucleotide 1076 relative to the start codon in pU158 by PCR using UO121 and UO122 (see Table S1 at <http://candida.bri.nrc.ca/papers/myo/>). The green fluorescent protein (GFP) sequence was PCR amplified with UO105 and UO127, and to generate pU165, the 700-bp PCR product was cloned as a SalI-NsiI fragment into the 8.9-kb PCR product consisting of *RVS167* in pVEC. Several clones were verified by sequencing, and one difference was observed between our cloned *RVS167* sequence and the one available in the Stanford sequence database (<http://www-sequence.stanford.edu/group/candida>): K87T.

The *GFP-GSCI* construct was made by PCR amplification using UO133 and UO134 with genomic DNA as a template. The 1.4-kb PCR product comprising the promoter and 5' coding region was cloned into pBluescript SK as a SacI-XbaI fragment (pU181). The BamHI site was removed by filling in with Klenow followed by religation (pU184). New NotI and BamHI sites were introduced right after the ATG in pU184 by PCR using UO141 and UO142. The GFP sequence was PCR amplified with UO132 and UO143, and to generate pU187, the 700-bp PCR product was cloned as a NotI-BamHI fragment into the 4.4-kb PCR product consisting of the 5' end of *GSCI* in pBS. Several clones were verified by sequencing. Finally, the 2.1-kb SacI-XbaI fragment from pU187 was subcloned into pVEC to generate pU191.

Phenotypic analyses. Strains were tested for calcofluor white (50 μg/ml) and zymolyase (100 μg/ml) sensitivity as described by Marcus et al. (24). Cells were also tested for heat shock resistance at 48°C for 10, 20, 30, and 60 min, as well as for osmotic sensitivity on 1.0 M NaCl, 1.5 M NaCl, and 1.2 M sorbitol yeast extract-peptone-dextrose (YPD) plates (24).

Fluorescence microscopy. Cultures of the various strains grown overnight in YPD were diluted 1:20 in YPD supplemented with 10% fetal bovine serum and grown for 1 to 2 h at 37°C. Rhodamine-phalloidin (Molecular Probes, Eugene, Oregon) and calcofluor white (Sigma) staining was done as described by Oberholzer et al. (41). Cytochalasin A was added where indicated to a final concentration of 5 μM. Staining of lipid rafts with filipin III (Sigma) was done as described previously (36), as was the procedure for visualizing FM4-64 uptake (54).

To obtain mutant and wild-type strains expressing *RVS167-GFP* and *GFP-GSCI*, Ura⁻ strains were transformed with 10 μg of pU165 linearized with BglIII and with an 8.4-kb fragment obtained by PCR amplification of pU191 using UO156 and UO157. Transformants were screened for the expression of Rvs167-GFP and GFP-Gsc1 by epifluorescence and/or Western blot analysis. Cells expressing Rvs167-GFP and GFP-Gsc1 were grown to saturation in synthetic dextrose (SD)-Ura medium and diluted 1:20 in SD-Ura medium supplemented with 10% fetal bovine serum. Cells were then incubated for 90 min to 2 h at 37°C before being mounted directly on slides and visualized by epifluorescence microscopy using a Leica-DM-IRB inverted microscope with a 63× objective and a 10× projection lens. Pictures were acquired with a Sensys charge-coupled-device camera by use of Openlab 3.1 software.

Disruption of HOG1 and MKC1. The *HOG1* and *MKC1* genes were deleted in the *myo5Δ* and/or CAI4 backgrounds by use of PCR-amplified disruption cassettes. For disruption of *HOG1*, PCR was performed using oligonucleotides UO186 (5'ATTTTAAACAAGTTATAGAAAAGAAAATTTTCAAGAAGATAAAGCATATAAGAAAATGTCTGCAGATGGAGAATTTACAAGAACCGTAAAACGACGGCCAG3') and UO187 (5'CTTTTAAATTTTCTATAA TTGCTAGCTTGTATTTTGAAGATTAAGCTCCGTTGGCGGAATCCAA GTTGTTTTGCTCCGGAACAGCTATGACCATG3') to amplify a 2.0-kb fragment from pBS-URA3, a kind gift from Catherine Bachewich, and oligonucleotides UO210 (5'TTCAAGTCGTCTTTGAAAACATACACCGTGAATA ATAACAACAACATTTTAAACAAGTTATAGAAAAGAAAATTTTACAA AGATAAAGCATATAAGAAAACCCGGGATGCTGATAGAGC3') and UO211 (5'ATGCTCCCATCCACGGGATTTAGCTCAGTGTATCTATTTGGTGA TTTCAAAAACAGTCCCAAAATCTGGGTTCTTTGTAATTTCCATCT GCAGACATATCCGGTAATTTAGTGTG3') to amplify a 2.4-kb fragment from pSAT-tet (47). PCR products were purified using a QIAquick PCR kit. Four PCRs were pooled, ethanol precipitated, and used for transformation of strains COU46 and CAI4. Transformants for the deletion of the first allele were selected on SD-Ura plates and screened by colony PCR using oligonucleotides UO194 (5'CGGACTAGTGGCACTAAACATCAATTTCC3') and UO196 (5'ATAATCGCTGTGCTACTGGTGAG3'). Transformants for both alleles deleted were grown in YPD for 1 day before selection on SD-Ura plates supplemented with nourseothricin, 200 μg/ml, and screened by colony PCR using UO194 and UO205 (5'CACCGAAATTTTCATGGATCC3').

For disruption of *MKC1*, PCR was performed using oligonucleotides UO214 (5'AACTGAAACCCAAAAAATTTTCTTGTCTACTACTAGT TGTCTTTTAAACTTTCTCTTGAACAGCAGTTTTATAAAGAACCAA TTTCATAGGAAACAGCTATGACCATG3') and UO187 (5'AAAAGGAG GTACTAAAGGTCAATATATATAAACCACCCTAATGGATAGAGT AATTCCGAGAGTAACATACCCCGGGATAACGTTGTGTGTTTCAA GTAAAACGACGGCCAGT3') to amplify a 2.0-kb fragment from pBS-URA3 and oligonucleotides UO225 (5'AACTGAAACCCAAAAAATTTT TTTGCTACTACTAGTTGTCTTTTAAACTTTCTTGTGAAACAGCAGT TTTATAAAGAACCAATTTCCATACCCGGGATGCTGATAGAGC3') and UO226 (5'ACTCCTTGACTATTTTGAATCGACTATCAATGATAAATCC TGGTTGTAGACCTTATTTACGGATCTGCCATAATATATGGGTGCTTC TTGTTGATCCATATCCGGTAATTTAGTGTGTG3') to amplify a 2.4-kb fragment from pSAT-tet (47). PCR products were purified using a QIAquick PCR kit. Four PCRs were pooled, ethanol precipitated, and used for transformation of strain COU46. The *mkc1Δ* mutant strain was kindly provided by J. Plá. Transformants for the deletion of the first allele were selected on SD-Ura plates and screened by colony PCR using oligonucleotides UO217 (5'CTTCACGAG CATAACAAAATCAG3') and UO196. Transformants for both alleles deleted were grown in YPD for 1 day before selection on SD-Ura plates supplemented with nourseothricin, 200 μg/ml, and screened by colony PCR using UO217 and UO205.

All potential candidates were further tested for the correct integration events by Southern blotting. The absence of *MKC1* was confirmed by Southern blotting in the following way. Ten micrograms of genomic DNA for each strain was digested with HindIII, separated on a 1% agarose gel, and transferred to Zeta-Probe nylon membranes (Bio-Rad). The DNA was then probed using radioactively ³²P-labeled PCR product amplified from genomic DNA from SC5314 using UO217 and UO228. This fragment corresponds to the 5' region of the *MKC1* open reading frame (nucleotide -191 to nucleotide +350). In addition, the absence of Hog1p was confirmed by Western blotting using α-p38 antibodies at a 1:1,000 dilution (Cell Signaling Technology, MA). Blots were also probed with α-actin MAB150 (Chemicon International, Temecula, CA) at a 1:1,000 dilution to control for loading.

Western blot analysis. Wild-type and mutant strains were grown in YPD to an optical density at 600 nm of 1.0 and treated with 0.5 M NaCl for 3 min. Cells were rapidly collected, washed with phosphate-buffered saline, and frozen. Whole-cell

extracts were obtained by glass bead beating the cells 10 times for 15 s each in 50 mM Tris-HCl, pH 7.5, 100 mM NaCl, 1 mM EDTA, 0.1% Triton X-100, and 25 mM NaF supplemented with protease inhibitors. Extracts were cleared by centrifugation at $9,800 \times g$ for 2 min, and 10 μ l was loaded on 8% sodium dodecyl sulfate (SDS)-polyacrylamide gels. Phosphorylation levels of Hog1 were detected by Western blotting using anti-phospho p38 (Cell Signaling Technology, MA) at a 1:1,000 dilution.

Probes, chip hybridization, and quantification. Most of the transcript profiling in this study used Cy3- and Cy5-labeled cDNA probes that were produced from approximately 3 to 5 μ g of poly(A)(+) RNA and hybridized, as described previously, to microarrays spotted with amplicons from 6,002 putative open reading frames (39). For each condition, at least three independent experiments with reciprocal labeling were done, for a total of six individual hybridizations, unless otherwise stated. Transcript profiles of the *myo5* Δ vs. wild type (Wt), *mkc1* Δ vs. Wt, and *myo5 mkc1* Δ vs. *myo5* Δ mutants, described in the latter part of this report, were produced with Cy3- and Cy5-labeled cDNA probes prepared from 40 μ g of total RNA and hybridized to a new generation of long oligonucleotide microarrays. These were spotted with 6,263 70-mer oligonucleotides that are specific for genes recently identified as part of a reannotation of the *C. albicans* genome (10). More details about these microarrays are available on our web page at http://www.bri.nrc.gc.ca/services/microarray/scanning_e.html. The latter profiling data are the result of four hybridizations of independently produced RNA preparations.

All microarrays were washed in $1 \times$ SSC ($1 \times$ SSC is 0.15 M NaCl plus 0.015 M sodium citrate) and 0.2% SDS at 42°C followed by two washes in $0.1 \times$ SSC and 0.2% SDS at 42°C and finally three quick consecutive washes in $0.1 \times$ SSC. Chips were air dried before being scanned with a ScanArray Lite microarray scanner (Packard Bioscience). QuantArray was used to quantify fluorescence intensities, and Lowess normalization and statistical analysis were performed using GeneSpring v.7 (Agilent Technologies, CA). The microarray data produced in this study are available on our web page at <http://candida.bri.nrc.ca/papers/myo/>. The data can also be found in the supplemental material on the Eukaryotic Cell web page (<http://ec.asm.org/>).

Northern blot analysis. Total RNA was extracted with phenol and glass beads from wild-type and myosin I deletion strains grown to early log phase in YPD at an optical density at 600 nm of 0.8. Twenty micrograms of total RNA per sample was separated on a 7.5% formaldehyde, 1% agarose gel, blotted onto Zeta-Probe nylon membrane (Bio-Rad, Ontario, Canada), and probed with 32 P-labeled DNA specific for *ACT1* (*orf19.5007*), *orf19.5302*, *CRH1* (*orf19.2706*), *AGP2* (*orf19.4679*), *orf19.7296*, *SOD5* (*orf19.2060*), *EBP1* (*orf19.125*), *PHR1* (*orf19.3829*), and *TOS2* (*orf19.1911*) as described previously (42). All Northern probes were PCR products subsequently labeled by random priming (Amersham Biosciences, NJ). Oligonucleotides used were UO106 and UO107 (*ACT1*), UO238 and UO239 (*orf19.5302*), UO240 and UO241 (*orf19.7296*), UO242 and UO243 (*EBP1*), UO244 and UO245 (*CRH1*), UO246 and UO247 (*PHR1*), UO248 and UO249 (*AGP2*), and UO252 and UO253 (*TOS2*) (see Table S1 at <http://candida.bri.nrc.ca/papers/myo/>). The *SOD5* PCR product was kindly provided by M. Martchenko.

RESULTS

***myo5* Δ and *sla2* Δ mutants display endocytic defects.** In *C. albicans*, perturbations in the actin cytoskeleton are coupled to defects in hyphal development. For example, myosin I function is important for proper cortical actin patch distribution and for endocytosis and is critical for the formation of true hyphae (41, 42). The *sla2* Δ mutant also exhibits defects in both hyphal formation and the organization of cortical actin patches (5) (see Fig. S1A at <http://candida.bri.nrc.ca/papers/myo/>). Chemical treatments that disrupt the actin cytoskeleton, such as cytochalasin A treatment, can also modify hyphal development and cortical actin patch distribution (1) (see Fig. S1A at <http://candida.bri.nrc.ca/papers/myo/>). Correlating with these actin cytoskeleton defects, the *myo5* Δ and *sla2* Δ mutations, as well as cytochalasin A treatment, also negatively affect fluid-phase endocytosis (see Fig. S1B at <http://candida.bri.nrc.ca/papers/myo/>).

However, not all defects in cortical actin distribution cause

such pleiotropic effects. Deletion of the Src homology 3 (SH3) and A domains of myosin I (the Δ SH3 Δ A mutant) affects the organization of the actin cytoskeleton but neither fluid-phase endocytosis (see Fig. S1A and S1B at <http://candida.bri.nrc.ca/papers/myo/>) nor hyphal development. The Δ SH3 Δ A mutant is particularly interesting because it is able to form apparently wild-type hyphae despite the highly depolarized distribution of cortical actin patches.

Clustering of the *myo5* Δ and *sla2* Δ transcript profiles. Unlike their *S. cerevisiae* counterparts, the *myo5* Δ and *sla2* Δ mutants of *C. albicans* are viable and exhibit only slight growth defects, indicating that the *MYO5* and *SLA2* genes do not play an essential role in *C. albicans*. Transcript profiles of *myo5* Δ and *sla2* Δ mutant cells grown under yeast (*myo5* Δ -Y and *sla2* Δ -Y, respectively)- or hypha-inducing conditions were obtained using whole-genome DNA microarrays and compared to transcript profiles of the wild type to gain insight into the physiological roles of Myo5p and Sla2p during vegetative and hyphal growth. Transcript profiles of Δ SH3 Δ A mutant cells grown under yeast and hyphal growth conditions as well as profiles of wild-type yeast and hyphal cells treated for 10 and 30 min with 5 μ M cytochalasin A were also obtained. Overall, transcript profiling was used as a tool to assess the similarities and differences among the different conditions and mutants.

Some 2,500 genes for which the transcript levels vary significantly ($P < 0.05$) under at least one condition tested were selected for further analysis. Principal component analysis (PCA) and hierarchical clustering show that, of all the conditions, the *myo5* Δ and *sla2* Δ transcriptional profiles of cells grown as yeast or hyphae are most similar (Fig. 1) (also see Fig. S2 at <http://candida.bri.nrc.ca/papers/myo/>). In contrast, treatment of cells with cytochalasin A or deletion of the SH3 and A regions of myosin I produce transcript profiles that do not cluster with each other or with any of the other profiles obtained. Thus, the common modified profiles represent those of the *myo5* Δ and *sla2* Δ endocytosis-defective mutants.

Even though the *myo5* Δ and *sla2* Δ mutants are defective in hyphal formation, the yeast-to-hypha transcript profiles of wild-type and mutant strains clustered together on the PCA graph (Fig. 1) because the changes in the yeast-to-hypha transcript profiles are only minimally altered in the *myo5* Δ and *sla2* Δ hyphal-formation-defective mutants. Thus, it appears that the physical state of the cells (pseudohyphae) does not preclude expression of hyphal-specific genes. Apparently the signal transduction pathways relaying the hypha-inducing environment to the transcriptional machinery were unaffected by the altered state of the *myo5* Δ and *sla2* Δ mutant cells. However, some hyphal-specific genes are not induced to the same level in the *myo5* Δ mutant as in the wild type under conditions that normally induce hyphae; these genes include *ECE1*, *GPXI*, and *YHB1* (data not shown). As well, the hyphal-specific *RNR3* gene was repressed in the *sla2* Δ mutants grown under hypha-inducing conditions (data not shown).

We observed a significant number of genes commonly affected in strains deleted for *SLA2* or *MYO5* by comparing the fluorescence ratios of significantly modulated transcripts in the *myo5* Δ and *sla2* Δ mutants relative to that of the wild type (Fig. 2) ($P < 1e-86$). Importantly, the changes (n -fold) of commonly modulated genes and even those that passed the significance test ($P < 0.05$) in one mutant but not the other were similar in

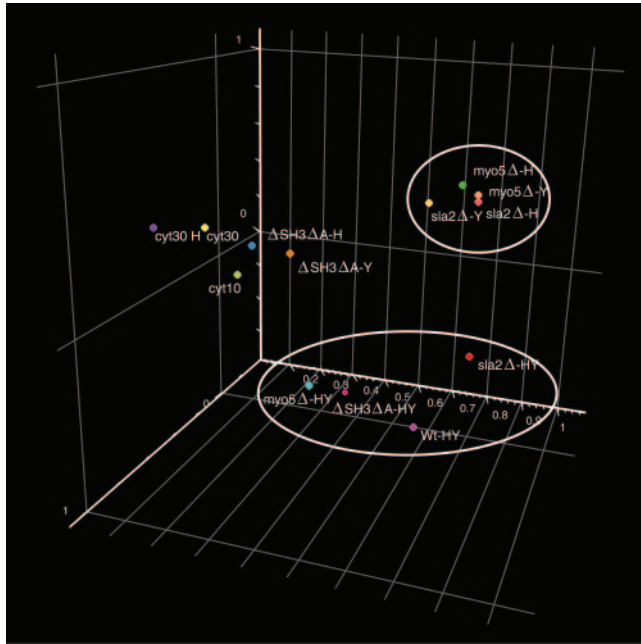


FIG. 1. PCA of the transcript profiles. This data reduction algorithm organizes the experimental conditions in a three-dimensional space based on the similarity between their respective transcriptional profiles. The conditions include comparing *myo5Δ*, *sla2Δ*, and Δ SH3 Δ A mutants against Wt cells under yeast (Y) or hyphal (H) growth conditions, comparing Wt and mutant strains grown under hyphal growth conditions to the same strains grown under yeast growth conditions (HY), treatment of Wt yeast cells with cytochalasin A for 10 or 30 min (cyt 10 and cyt 30, respectively), or treatment of hyphal cells with cytochalasin A for 30 min (cyt 30 H). White ovals denote clustering of conditions that are discussed in the text.

both mutants relative to the wild type. Many transcript levels that were increased in common also correspond to genes induced when wild-type cells are stressed osmotically (32%; $P < 1e-15$) (16) (Table 1). Among common transcripts with levels in the mutants less than $0.6\times$ or greater than $1.4\times$ the levels in the wild type, many encode cell wall components (12%), membrane proteins involved in protein sorting, trafficking, transport, and other functions (11%), and proteins involved in membrane biogenesis (6%) (Table 2). As well, many of these transcripts were stress-induced genes and genes involved in protein folding and degradation (9%). Table S2 at <http://candida.bri.nrc.ca/papers/myo/> shows transcript levels for genes that were significantly modulated in the *myo5Δ* mutant in two different types of DNA microarrays that were spotted with either PCR amplicons or 70-mer oligonucleotides, with the addition of some genes that appeared to be significant on only one type of chip, as indicated (see below). Importantly, none of these genes were modulated in control experiments comparing transcript profiles of *MYO5* and *SLA2* revertant strains with that of wild-type SC5314. The only exception is *IRO1*, which is found adjacent to the *URA3* gene that was deleted in the making of CAI4 (19). Accordingly, the transcript levels of *IRO1* are lower in all of the CAI4-derived strains than in SC5314 (data not shown). Table S1 at <http://candida.bri.nrc.ca/papers/myo/> also highlights the similar transcript patterns of *myo5Δ* and *sla2Δ* under yeast growth conditions (*myo5Δ*-Y and *sla2Δ*-Y) and especially those of *myo5Δ*-Y and *sla2Δ* under hyphal growth conditions.

Genes involved in membrane biogenesis and function are affected in *myo5Δ* and *sla2Δ* mutants. Transcript levels of several genes involved in membrane biogenesis, including

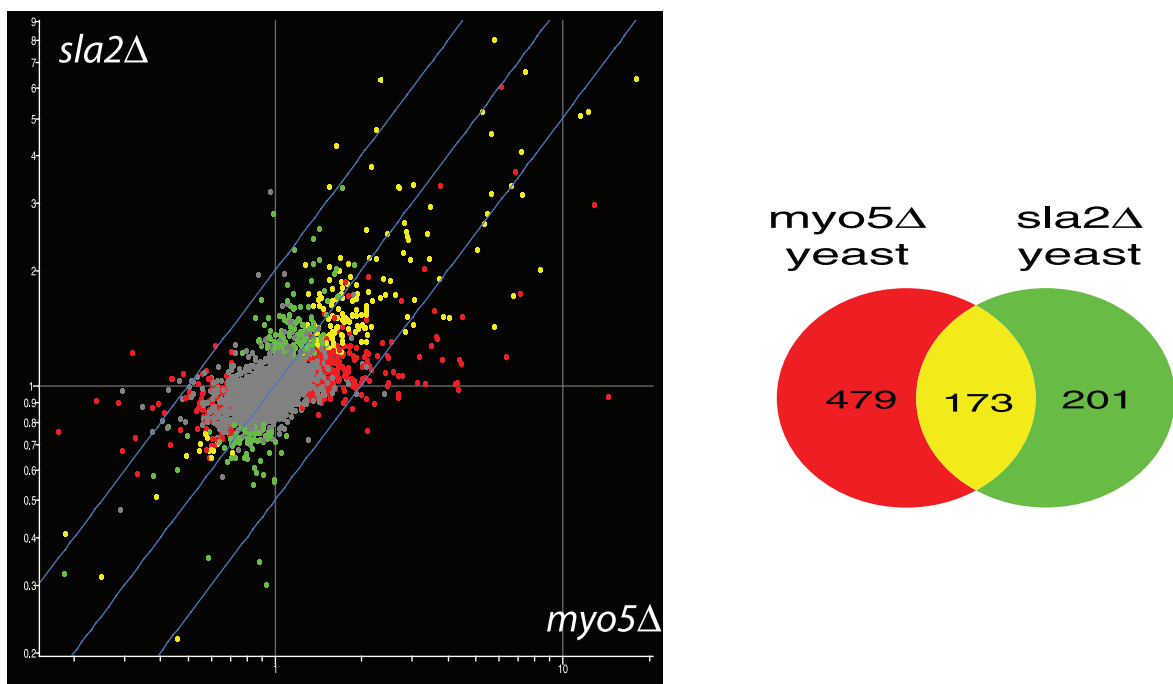


FIG. 2. Similarity between the transcript profiles of the *myo5Δ* and *sla2Δ* mutants. Shown is a scatter plot of the average fluorescence ratios observed under yeast growth conditions for *myo5Δ* versus *sla2Δ*. Transcripts with a statistically significant change in abundance (t test, $P < 0.05$, coupled to the Benjamini and Hochberg false discovery rate) are colored as indicated in the Venn diagram (red, *myo5Δ* transcripts; green, *sla2Δ* transcripts; yellow, overlap). The numbers in the Venn diagram indicate numbers of genes.

TABLE 1. Comparison of gene lists obtained under various conditions^a

Condition	No. (%) of <i>myo5Δ</i> mutant transcripts induced ^b	<i>P</i> value	No. (%) of <i>myo5Δ</i> -Y and <i>sla2Δ</i> -Y mutant transcripts induced ^c	<i>P</i> value	No. (%) of Cyt A ^d -treated gene transcripts induced	<i>P</i> value	No. (%) of Δ SH3 Δ A mutant transcripts induced
Osmotic stress	47 (33)	1.28e-18	45 (32)	2.85e-16	8 (15)		4 (14)
Oxidative stress	13 (9)	1.64e-4	11 (8)	1.35e-3	20 (36)	6.87e-8	5 (17)
Heat shock	13 (9)	8.17e-6	13 (9)		13 (24)	1.49e-4	3 (10)
Total ^e	143		141		55		29

^a Only lists of genes for which transcript levels were greater than 1.3 and *P* values were <0.05 under each of the conditions were compared.

^b Commonly identified transcripts with higher levels in the *myo5Δ* mutant, obtained using amplicon and oligonucleotide chips.

^c Commonly identified transcripts with higher levels in the *myo5Δ*-Y and *sla2Δ*-Y mutants.

^d Cyt A, cytochalasin A.

^e Total number of induced transcripts for each condition.

CHO1 and *SFK1* (membrane biogenesis), *RTA2*, *RTA3*, and *RTA4* (putative flippases), and *PLC2*, *PLC3*, and *PLB4* (phospholipases), were significantly modulated in both mutants (see Table S2 at <http://candida.bri.nrc.ca/papers/myo/>). Phospholipases and Sfk1p play an important role in intracellular signaling (6, 56). It is intriguing that three independent flippase genes are overexpressed in the mutants. Flippases are known to maintain an asymmetric distribution of sphingolipids in the extracellular leaflet of the lipid bilayer and may therefore play an important role in regulating endocytosis (31).

Because lipid rafts are membranous structures that may anchor and localize proteins in a polarized manner during *C. albicans* hyphal morphogenesis (36, 38), we assessed whether the endocytic mutant strains exhibited defects in lipid raft formation. We visualized the wild-type and mutant strains grown under hypha-inducing conditions stained with filipin III

for ergosterol, a component of lipid rafts. The hyphal tips of wild-type and Δ SH3 Δ A cells were heavily stained with filipin III, indicating that lipid rafts are polarized (Fig. 3). In contrast, the endocytic *myo5Δ* and *sla2Δ* mutants clearly lacked polarized lipid rafts under these conditions.

In *S. cerevisiae*, Rvs167p is a cortical actin patch component that interacts through its SH3 domain with multiple proteins, including Las17p/Bee1p (8, 52), which recently was found to be associated with lipid rafts (22). *C. albicans* *RVS167* was fused with *GFP*, immediately 3' of the BAR sequence, and intro-

TABLE 2. Classification of genes into functional categories^a

Function	No. (%) of transcripts induced			
	<i>myo5Δ</i> mutant ^b	<i>myo5Δ</i> -Y and <i>sla2Δ</i> -Y mutants ^c	Cyt A-treated genes ^d	Δ SH3 Δ A mutant ^e
Cell wall biogenesis	17 (11)	13 (16)	0 (0)	1 (4)
Membrane biogenesis	8 (5)	9 (11)	1 (2)	2 (4)
Membrane transport	7 (5)	3 (4)	5 (8)	3 (7)
Unknown membrane function	7 (5)	2 (2)	3 (5)	0 (0)
Protein trafficking and sorting	12 (8)	3 (4)	0 (0)	0 (0)
Endocytosis and actin elements	5 (3)	1 (1)	0 (0)	1 (2)
Multidrug resistance	0 (0)	1 (1)	3 (5)	2 (4)
Stress and redox	14 (9)	10 (12)	14 (23)	1 (2)
Protein folding and degradation	6 (4)	1 (1)	9 (15)	2 (4)
Iron metabolism	4 (3)	1 (1)	0 (0)	0 (0)
Metabolism	20 (13)	10 (12)	12 (19)	22 (42)
Miscellaneous	18 (12)	6 (7)	7 (11)	9 (16)
Unknown	33 (22)	21 (26)	8 (13)	8 (15)
Total	151	81	62	51

^a Table 2 is based on data presented in Tables S1, S2, and S3 at <http://candida.bri.nrc.ca/papers/myo/>.

^b Commonly identified transcripts in the *myo5Δ* mutant, obtained using amplicon and oligonucleotide microarrays.

^c Commonly identified transcripts in the *myo5Δ*-Y and *sla2Δ*-Y mutants.

^d Transcripts unique to cytochalasin A (Cyt A)-treated genes and not identified in the *myo5Δ* and *sla2Δ* mutants.

^e Transcripts unique to the Δ SH3 Δ A mutant and not identified in the *myo5Δ* and *sla2Δ* mutants; these may also have been identified under cytochalasin A treatment conditions.

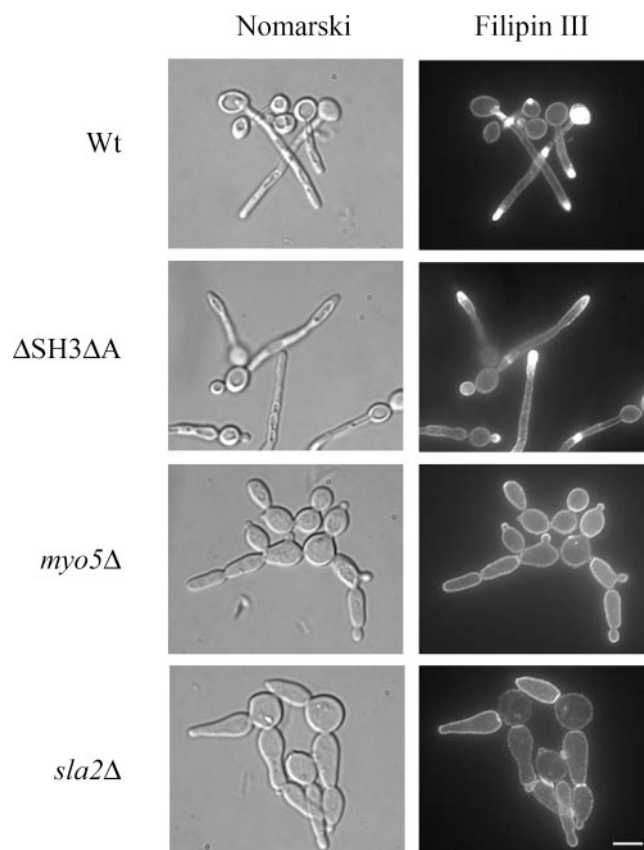


FIG. 3. The *myo5Δ* and *sla2Δ* mutants do not exhibit polarized lipid rafts. The wild-type and mutant cells grown under hypha-inducing conditions were stained with filipin III and visualized by epifluorescence microscopy. Bar = 5 μ m.

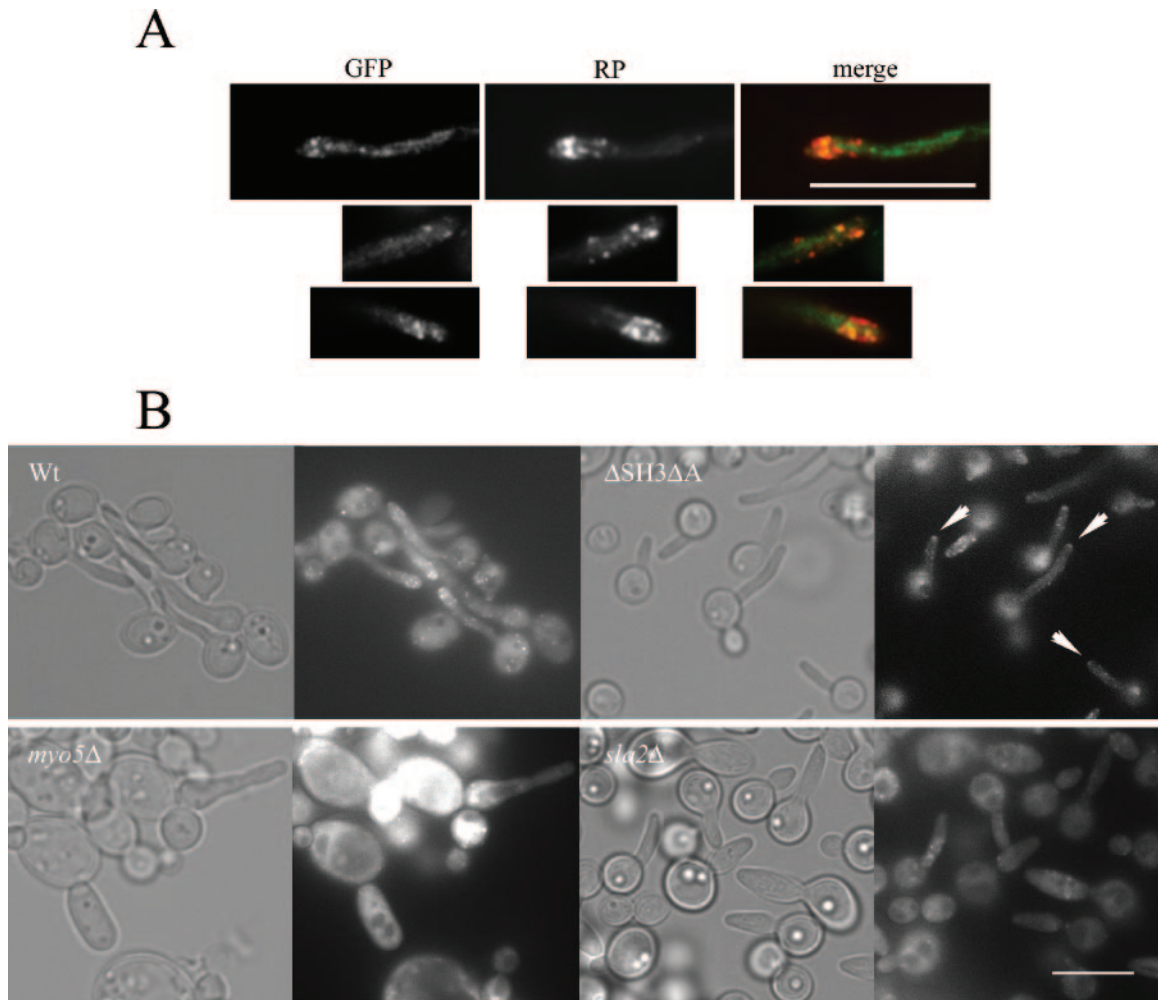


FIG. 4. Rvs167-GFP does not localize in a polarized manner in the *myo5Δ* and *sla2Δ* mutants. (A) Partial colocalization of Rvs167p-GFP with cortical actin patches in wild-type hyphal tips. Hyphal cells expressing Rvs167p-GFP were fixed, stained with rhodamine-phalloidin (RP), and visualized by epifluorescence microscopy. (B) Wild-type and mutant hyphal forms expressing Rvs167p-GFP were visualized by epifluorescence microscopy. Arrowheads point to mutant hyphal tips showing Rvs167-GFP signal. Bar = 10 μ m.

duced into wild-type and mutant strains. The Rvs167p-GFP levels expressed in these strains were examined by immunoblot analysis (data not shown) and localized by epifluorescence microscopy. Rvs167p-GFP localized in patches at hyphal tips of wild-type cells, and these Rvs167p-GFP patches partially overlapped with cortical actin patches (Fig. 4A). Non-actin-overlapping Rvs167p-GFP patches may colocalize with lipid rafts. In the hyphal-formation-defective *myo5Δ* and *sla2Δ* mutants, Rvs167-GFP was mainly cytoplasmic, with some patches visible in the *sla2Δ* mutant (Fig. 4B). However, a distinct Rvs167p-GFP signal could be observed at hyphal tips of the Δ SH3 Δ mutant cells (Fig. 4B). The majority of these mutant hyphae had Rvs167p-GFP signal at the tip (77% [$n = 151$] of hyphal cells of the Δ SH3 Δ mutant, compared to 80% [$n = 97$] in the wild type). It is possible that Rvs167p-GFP localization at hyphal tips corresponds to polarized lipid rafts.

Genes involved in cell wall remodeling are affected in *myo5Δ* and *sla2Δ* mutants. Transcript levels of several genes encoding cell wall remodeling enzymes were elevated in the *myo5Δ* and *sla2Δ* mutants. These included genes involved in chitin synthe-

sis (*CHS2* and *CHS7*), in β -1,6-glucan assembly (*KRE1*, *KRE6*, *KRE7*, *KRE9*, and *KRE13*), and in β -1,3-glucan assembly (*orf19.7214*, *BGL2*, *EXG1*, and *XOG1*). In addition, transcript levels of several cell wall proteins that may have a role in cell wall assembly, such as glycosylphosphatidylinositol-anchored proteins (*PHR1* and *DCW2*), cell wall mannoprotein *CCW14*, and others (*CRH1* and *ECM4*), were increased in the *myo5Δ* and *sla2Δ* mutants. In contrast, *CHT2* and *CHT3* transcript levels were decreased in the *myo5Δ* mutant. This changed transcript pattern may be linked to thickening of the cell wall observed as an aberrant calcofluor staining of the cell wall of the *myo5Δ* and *sla2Δ* mutants but not of the wild-type and Δ SH3 Δ strains (Fig. 5) (41). We also assessed cell wall defects by monitoring resistance to 50 μ g/ml calcofluor and 0.05% SDS (see below). Consistent with a cell wall defect, we found that the *myo5Δ* and *sla2Δ* mutants were more sensitive to calcofluor and SDS than either the wild-type or the Δ SH3 Δ strain (Fig. 6).

Elevated levels of glucan and chitin synthases may cause a thickening of the cell wall in the *myo5Δ* and *sla2Δ* mutants. In

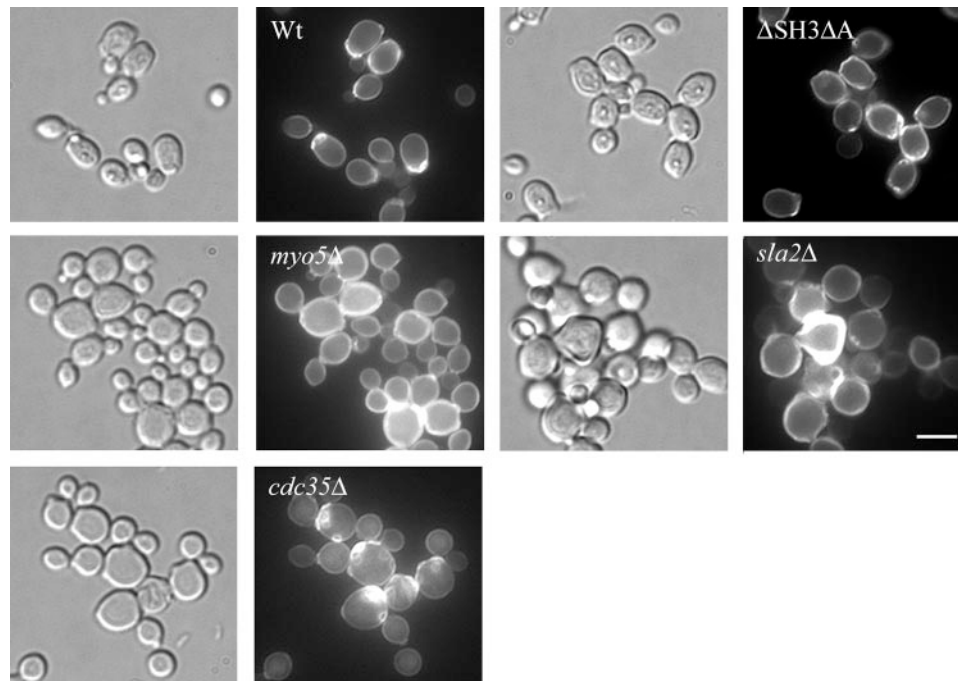


FIG. 5. Aberrant chitin depositions in the cell walls of *myo5Δ* and *sla2Δ* mutant cells. Wild-type and mutant cells were fixed, stained with calcofluor white, and visualized by epifluorescence microscopy. Bar = 5 μ m.

addition, a thicker cell wall could arise because of inefficient recycling of cell wall synthesizing proteins at sites of polarized growth, resulting in uniform localization around the cell wall. To assess such a defect, we introduced GFP-tagged β -1,3-glucan synthase Gsc1p (37) and visualized its localization in all strains. We found that GFP-Gsc1p was polarized to the hyphal tips of wild-type and Δ SH3 $\Delta\Delta$ cells (Fig. 7). In contrast, the GFP-Gsc1p signal was more diffuse in the *sla2Δ* mutants and greatly dispersed around the cell periphery in the *myo5Δ* mutant. Thus, these results show that these mutants exhibit secondary defects in cell wall assembly, possibly as a consequence of defective endocytosis and elevated transcript levels of cell wall remodeling genes.

The *myo5Δ* and *sla2Δ* mutants are more stress sensitive than the wild-type and Δ SH3 $\Delta\Delta$ strains. Analysis of the transcript profiles showed that the *myo5Δ* and *sla2Δ* mutants expressed high transcript levels for stress genes such as *DDR48*, *HSP12*, and *SOD5*, suggesting that the mutants are stressed. We determined whether these mutants had modified stress responses by performing spot test assays on media containing different salts and 0.05% SDS, on 50 μ g/ml calcofluor-containing plates, or following heat shock treatment of differing times at 48°C (Fig. 6). We observed that the *myo5Δ* and *sla2Δ* null mutants exhibited increased salt, SDS, calcofluor, and heat shock sensitivities compared to the wild-type and Δ SH3 $\Delta\Delta$ strains, suggesting that the form of constitutive stress they

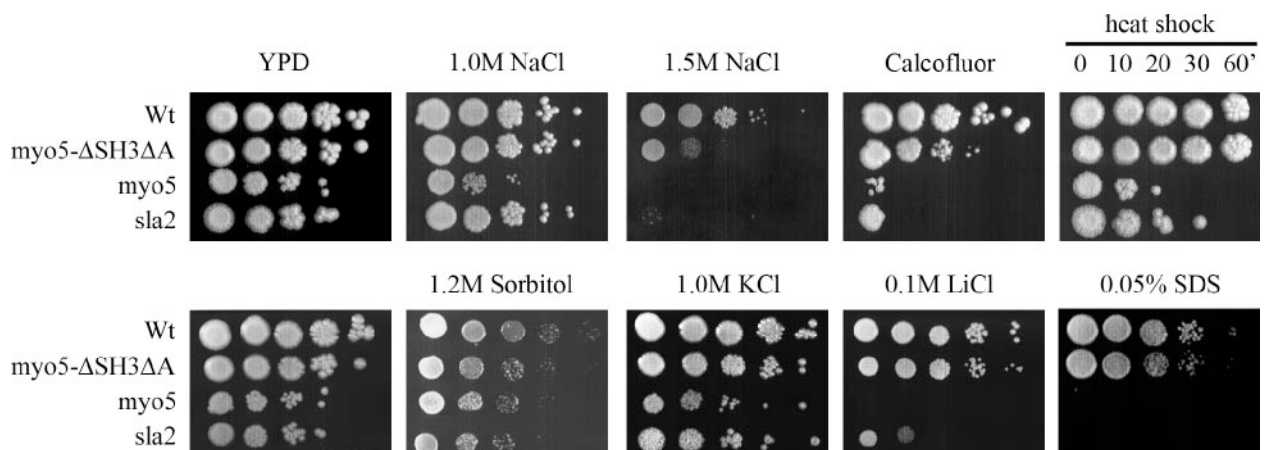


FIG. 6. The *myo5Δ* and *sla2Δ* mutants exhibit increased sensitivity to various stresses. Tenfold dilutions of overnight cultures of wild-type and mutant strains were spotted on various solid media as indicated and grown for 3 days at 30°C.

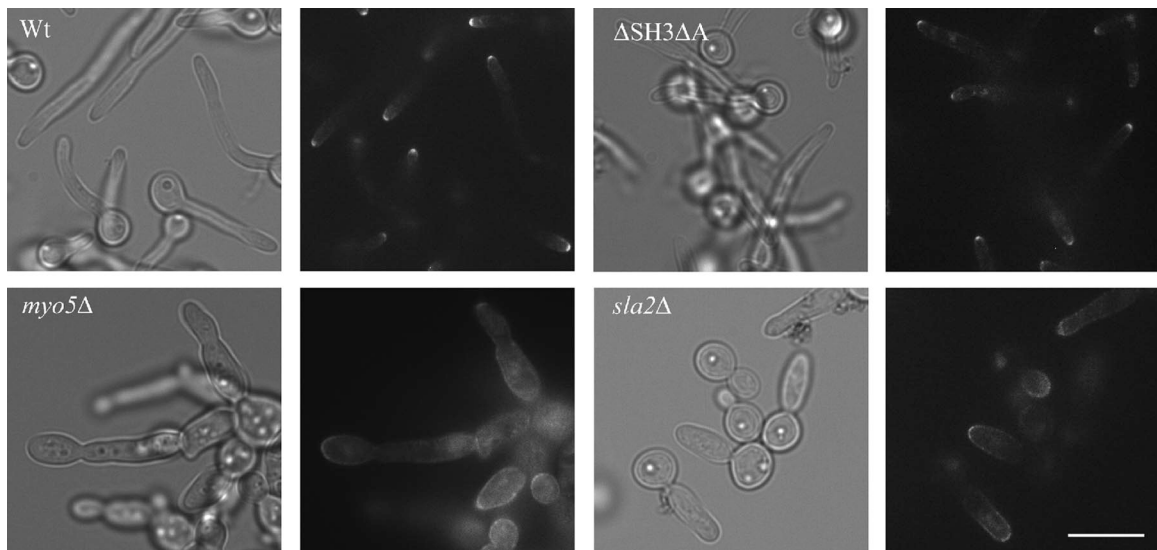


FIG. 7. Depolarized localization of GFP-Gsc1p in cell walls of *myo5Δ* and *sla2Δ* mutants. Wild-type and mutant cells grown under hypha-inducing conditions expressing GFP-Gsc1p were visualized by epifluorescence microscopy. Bar = 10 μ m.

experience does not cross-protect them against additional exogenous stress. In addition, these results suggest that misorganization of the cortical actin cytoskeleton per se, as in the Δ SH3 Δ A mutant, does not disturb resistance to stress.

Transcript profiles for the Δ SH3 Δ A mutant and wild-type cells exposed to cytochalasin A treatment were different from those of the *myo5Δ* and *sla2Δ* mutants. The transcript profiles of wild-type cells treated with cytochalasin A, a drug that inhibits polymerization of actin filaments, or of cells expressing a mutant form of Myo5p (Δ SH3 Δ A mutant) were different both from those of the *myo5Δ* and *sla2Δ* null mutants and from each other (Fig. 1) (compare transcript levels for these conditions in Table S2 at <http://candida.bri.nrc.ca/papers/myo/> with those of *myo5Δ*-Y). Importantly, 36% of genes uniquely up-regulated by cytochalasin A treatment were oxidative stress genes (Table 1) (16). Among the genes up- or downregulated by cytochalasin A, 5% encode multidrug resistance pumps, 23% encode stress genes, and 15% encode protein folding and degradation genes (Table 2). More specifically, cytochalasin A-treated cells had elevated transcript levels for genes encoding multidrug resistance pumps Mdr1p, Cdr1p, and Cdr2p and stress proteins Hsp70p, Sba1p, and Grp3p (see Table S3 at <http://candida.bri.nrc.ca/papers/myo/>). Of interest, we noted that the transcript levels for the Cap1p transcription factor involved in the oxidative stress response (17, 61) were up by two-fold. Transcript levels for a number of genes encoding oxidoreductases and dehydrogenases, including *OYE2*, *OYE32*, *GPX2*, *EBP1*, and putative dehydrogenase *orf19.3139*, were up accordingly in these cells. Transcript profiling of wild-type cells treated with cytochalasin A for 150 min shows that most elevated transcript levels at the 30-min condition returned to basal levels (data not shown). This indicates that even longer treatment of wild-type cells with cytochalasin A, which disorganizes the actin cytoskeleton and inhibits endocytosis more dramatically than a 30-min treatment, does not mimic an endocytosis defect generated by deletion of cortical actin patch components.

The Δ SH3 Δ A mutant had elevated or reduced transcript

levels for some genes commonly modulated in the myosin I null mutant. However, the transcript levels for common genes were clearly reduced overall and the number of genes uniquely modulated in this mutant was limited to a few (see Table S3 at <http://candida.bri.nrc.ca/papers/myo/>). These observations, together with the actin patterns observed for these cells, suggest that misorganization of the cortical actin patches alone is not sufficient to produce the specific transcriptional response observed in the case of the *sla2Δ* and *myo5Δ* endocytic mutants.

Phosphorylation of Hog1 is not involved in regulating transcript levels in the *myo5Δ* and *sla2Δ* mutants. The induction of genes by osmotic stress (and general stress) in the *myo5Δ* and *sla2Δ* mutants suggests that the osmotic stress response pathway is activated in these mutants (Table 1). In fact, there is considerable overlap between the lists of significantly modulated transcripts in *myo5Δ* or *sla2Δ* cells and wild-type cells treated with an osmotic shock ($P < 1e-30$ and $P < 1e-15$, respectively). The *C. albicans* Hog1 protein kinase is part of the p38 family and mediates signaling in response to a wide variety of stresses, including high salt and H₂O₂ concentrations, but not in response to heat shock (50). In *S. cerevisiae*, Hog1p mediates signaling in response to hyperosmotic stress. Hog1p receives signals from two independent branches that sense hyperosmotic changes in the environment. Activation of either the Sho1p-Ste11p or the Sln1p-Ssk1p branch or both leads to phosphorylation and activation of scaffold protein kinase Pbs2p, followed by phosphorylation, activation, and nuclear translocation of Hog1p (43). *C. albicans* Hog1p is similarly phosphorylated and translocated to the nucleus as part of the response (50). The long-term adaptation to hyperosmotic stress involves a change in transcriptional expression mediated by Hog1p phosphorylation of several transcription factors, including Sko1p, Hot1p, and Smp1p (2, 3, 12, 44).

We therefore determined whether Hog1p is constitutively phosphorylated in the *myo5Δ* and *sla2Δ* mutants in the absence of salt stress. Figure 8A shows that Hog1p became phosphorylated in wild-type cells exposed to 0.5 M NaCl for 3 min but

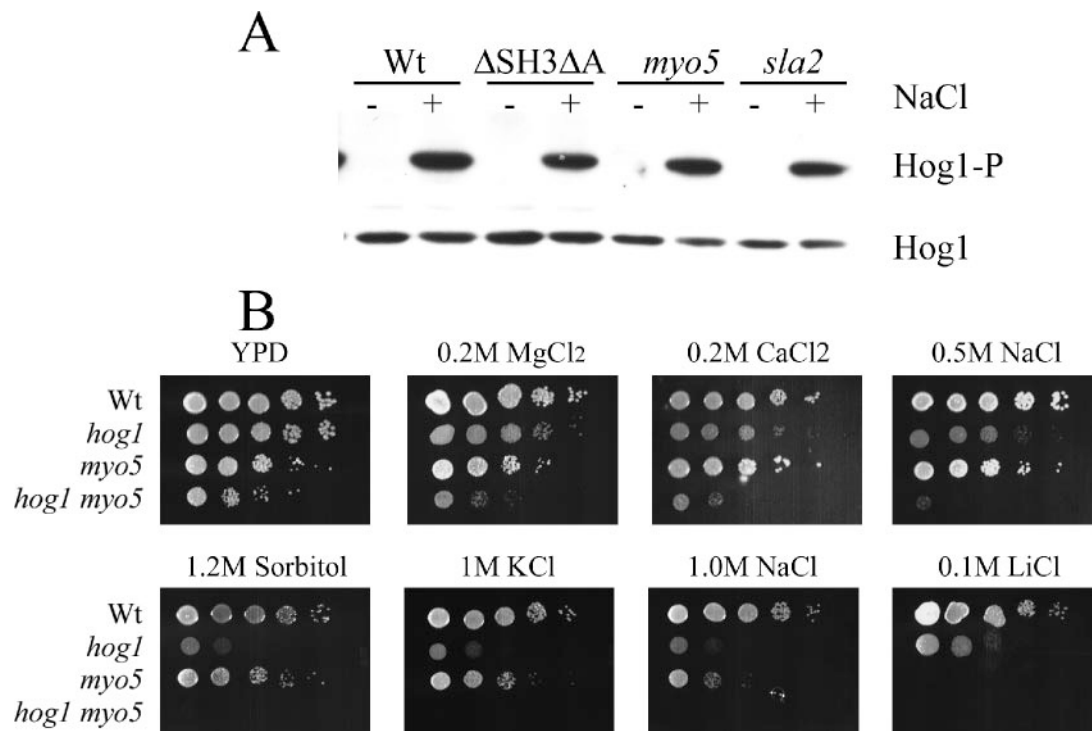


FIG. 8. (A) Hog1p is not phosphorylated in the *myo5* Δ and *sla2* Δ mutants grown in YPD but becomes phosphorylated when cells are treated with NaCl. Phospho-Hog1p was detected by Western blot analysis in wild-type and mutant strains grown in YPD (-) and stressed with 0.5 M NaCl for 3 min (+), using anti-phospho p38 antibodies. Hog1p protein levels were also detected using anti-p38 antibodies. (B) The *hog1* Δ and *myo5* Δ strains exhibit different salt sensitivities. Tenfold dilutions of overnight cultures of wild-type, *hog1* Δ , *myo5* Δ , and *hog1 myo5* Δ strains were spotted on solid medium containing various salts.

that Hog1p phosphorylation was not detected in the *myo5* Δ and *sla2* Δ mutants grown in YPD, suggesting that Hog1p is not constitutively activated in these mutants. Moreover, the salt sensitivity observed with the *myo5* Δ and *sla2* Δ mutants cannot be due to improper activation of the high-osmolarity pathway because phosphorylation of Hog1p occurred normally in these mutants when exposed to salt and because the salt sensitivities of the *hog1* Δ and *myo5* Δ mutants were different as determined by spot test assays (Fig. 8B).

To further address the requirement for the high-osmolarity stress response MAPK pathway in the transcriptional response of the *myo5* Δ mutant, we deleted the *HOG1* gene in the *myo5* Δ mutant background. Surprisingly, the *myo5 hog1* Δ double mutant grew poorly compared to single mutants and the wild type, suggesting that Hog1p is required when Myo5p is absent (Fig. 9A). Examination of *myo5 hog1* Δ cells revealed that many were abnormally enlarged and formed pseudohyphae despite being cultured in non-hypha-inducing conditions (data not shown). Transcript profiling of the *myo5 hog1* Δ double mutant compared to the *myo5* Δ single mutant revealed that the induction of 12 genes in the *myo5* Δ mutant was dependent on the presence of Hog1. These genes include *AGP2*, *CRH1*, *SOU1*, *orf19.5302*, and *orf19.7296* (see Table S2 at <http://candida.bri.nrc.ca/papers/myo/>). Northern blot analyses confirmed that elevated transcript levels for *AGP2*, *CRH1*, *orf19.5302*, and *orf19.7296* in the *myo5* Δ mutant are dependent on Hog1p (Fig. 10, left panel).

The transcript levels of a distinct set of genes affected by the deletion of *MYO5* are dependent on the Mkc1 protein kinase. As described above, the transcript levels of genes encoding cell wall organization and biogenesis proteins are affected by deletion of *MYO5* or *SLA2*. The transcript levels for many of these are induced when *S. cerevisiae* wild-type cells are exposed to chemical challenges to the cell wall (9, 20). These observations, together with the observed sensitivity of the *myo5* Δ and *sla2* Δ mutants to SDS and calcofluor, suggest that the cell wall integrity pathway is differentially modulated in these mutants. The elevated *PLC2* and *PLC3* transcript levels and repressed *PLB4* transcript levels observed for these mutants also suggest that intracellular signaling via the phosphoinositol secondary messenger may be activated. In mammalian cells this typically leads to the activation of Pkc1p, although this has not been demonstrated to occur in yeast (56). Activation of the Pkc1p cell wall integrity pathway in *S. cerevisiae* involves the phosphorylation of the MAPK Slt2p (13, 35).

To address the requirement of the Pkc1p cell wall integrity pathway for the mRNA transcript profiles observed for the *myo5* Δ and *sla2* Δ mutants, we deleted the *C. albicans* homologue for *SLT2*, *MKC1*, in the *myo5* Δ mutant. The double mutant had a clear growth defect (Fig. 9B). For the data generated in this section, we used newly designed long oligonucleotide microarrays (see Materials and Methods). The transcript profiles for the *myo5* Δ mutant and the wild type under yeast growth conditions generated with the cDNA and oligo-

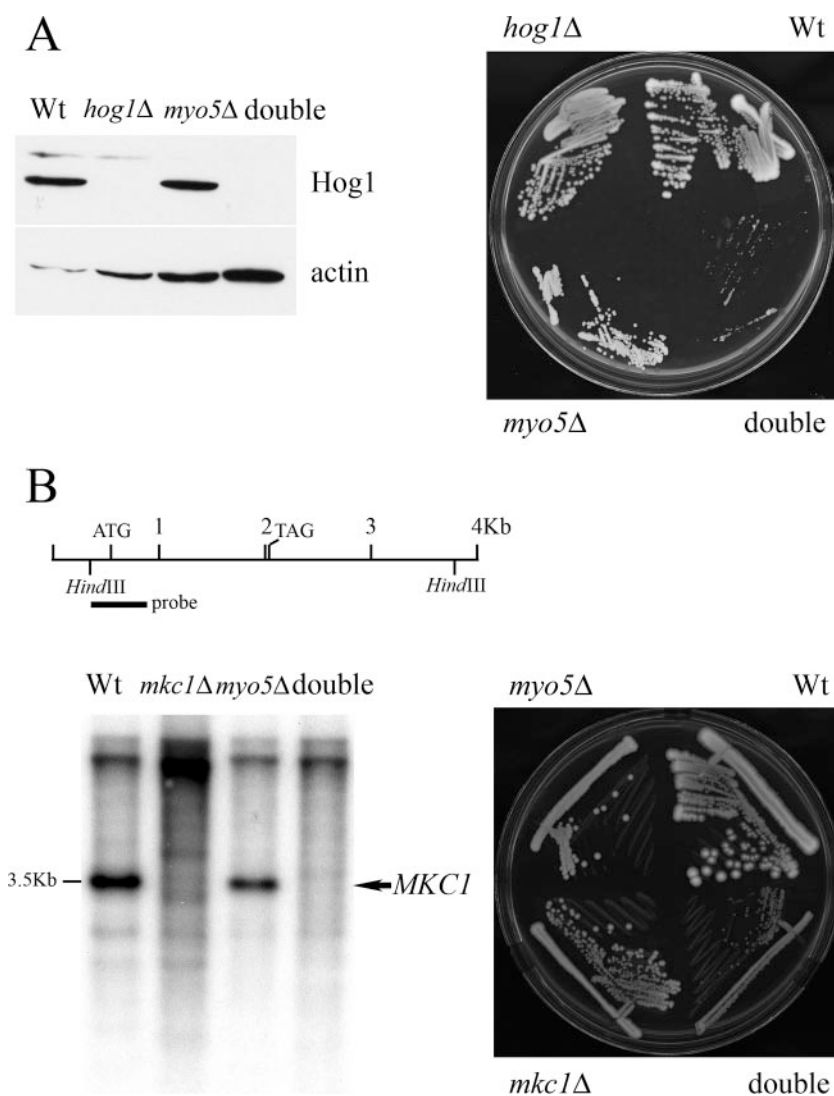


FIG. 9. Growth defect of *hog1 myo5Δ* and *mkc1 myo5Δ* double mutants compared to growth of single mutants. (A) The left panel shows the absence of Hog1p in the *hog1Δ* and *hog1 myo5Δ* strains by Western blotting using anti-p38 antibodies. The right panel shows colonies of the corresponding strains grown for 3 days on YPD at 30°C. (B) The left panel shows the absence of the *MKC1* gene in the *mkc1Δ* and *mkc1 myo5Δ* strains by Southern blotting (see Materials and Methods). The right panel shows colonies of the corresponding strains grown for 3 days on YPD at 30°C.

nucleotide chips were compared (Fig. 11) (also see Table S4 at <http://candida.bri.nrc.ca/papers/myo/>). The profiles were remarkably similar, suggesting that the data sets are highly reproducible ($P < 0.05$). Analysis of the transcript profile of the *myo5 mkc1Δ* double mutant compared to that of the *myo5Δ* single mutant showed 21 genes whose elevated transcript levels in *myo5Δ* were dependent on the presence of *MKC1*. These included genes encoding cell wall proteins (seven genes), detoxification proteins (three genes: *EBP1*, *SOD5*, and *orf19.251*), and unknown proteins (six genes, including *orf19.5302*). We confirmed by Northern blot analysis that the transcript levels of six genes (*orf19.5302*, *CRH1*, *EBP1*, *SOD5*, *TOS2*, and *PHR1*) were entirely or partially dependent on *MKC1* (Fig. 10, right panel). *TOS2* (target of SBF-2) transcript levels in the *myo5 mkc1Δ* double mutant were examined despite the absence of chip data because SBF is a known target of the Mkc1p protein kinase. Surprisingly, very few homo-

logues of these genes are modulated when *S. cerevisiae* is challenged with calcofluor white or zymolyase, causing cell wall perturbations known to activate the Pkc1p-Slt2p signaling pathway (9, 20).

The transcript levels of a significant number of genes were upregulated in both the *myo5Δ* and the *mkc1Δ* strain but were not increased in the *myo5 mkc1Δ* double mutant, suggesting that a common pathway can be activated independently in both single mutants. These included genes whose transcript levels were dramatically upregulated in the *myo5Δ* and *sla2Δ* single mutants, such as *HSP12*, *RNH2*, *PRY4*, *RTA2*, *PLC2/3*, *DDR48*, *XOG1*, and *PST*.

DISCUSSION

In this study, we undertook a genome-wide analysis of the transcript profiles of the *C. albicans myo5Δ* and *sla2Δ* mutants

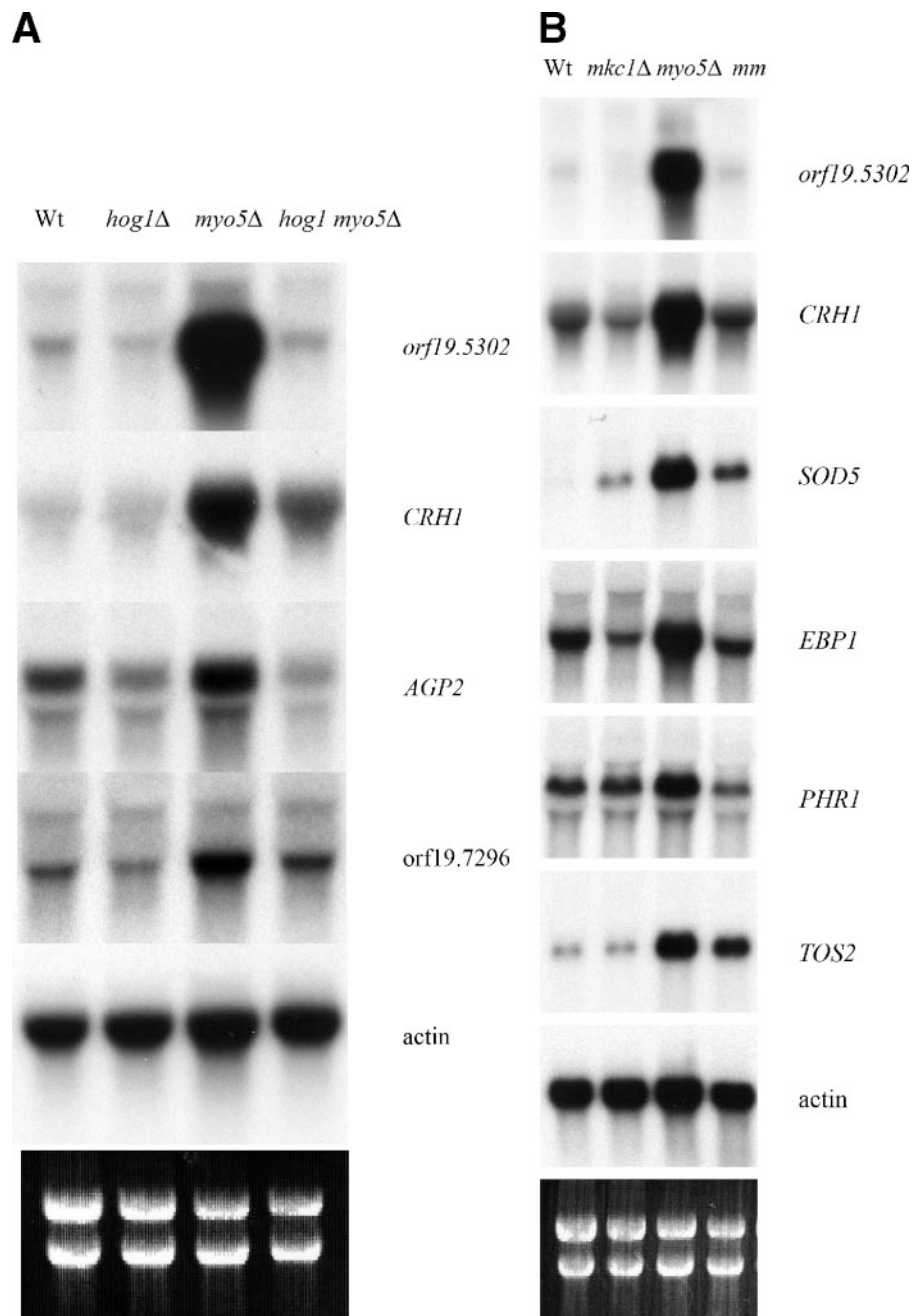


FIG. 10. The Hog1p and Mkc1p kinases are required for the elevated transcript levels of selected genes in the *myo5Δ* mutant strain. (Left panel) Northern blot analysis showing transcript levels for *orf19.5302*, *CRH1*, *AGP2*, *orf19.7296*, and *ACT1* in the strains shown at the top. (Right panel) Northern blot analysis showing transcript levels for *orf19.5302*, *CRH1*, *SOD5*, *EBP1*, *PHR1*, *TOS2*, and *ACT1* in the strains shown at the top. *mm*, *mkc1 myo5Δ* double mutant.

compared to that of the wild type under conditions promoting budding and hyphal growth to understand the physiological roles of the Myo5p and Sla2p proteins. Myo5p and Sla2p are involved in cortical actin patch function, and deletion of either gene caused very similar transcript profiles that included a dramatic and unexpected upregulation of stress-related genes and genes involved in cell wall remodeling and membrane biogenesis. This is the first time that an altered transcript profile has been observed for cortical actin skeleton mutants,

highlighting the complex adaptive response of mutants to their respective genetic defects. This altered transcript profile observed for the *myo5Δ* and *sla2Δ* mutants may be part of a response to compensate for endocytic-related defects, supporting the idea that endocytosis is critical for appropriate and timely expression of membrane and cell wall proteins during polarized growth. We interpret the cellular localization and distribution of the GFP-tagged glucan synthase (GFP-Gsc1p) in the *myo5Δ* and *sla2Δ* mutants, as discussed by Pruyne and

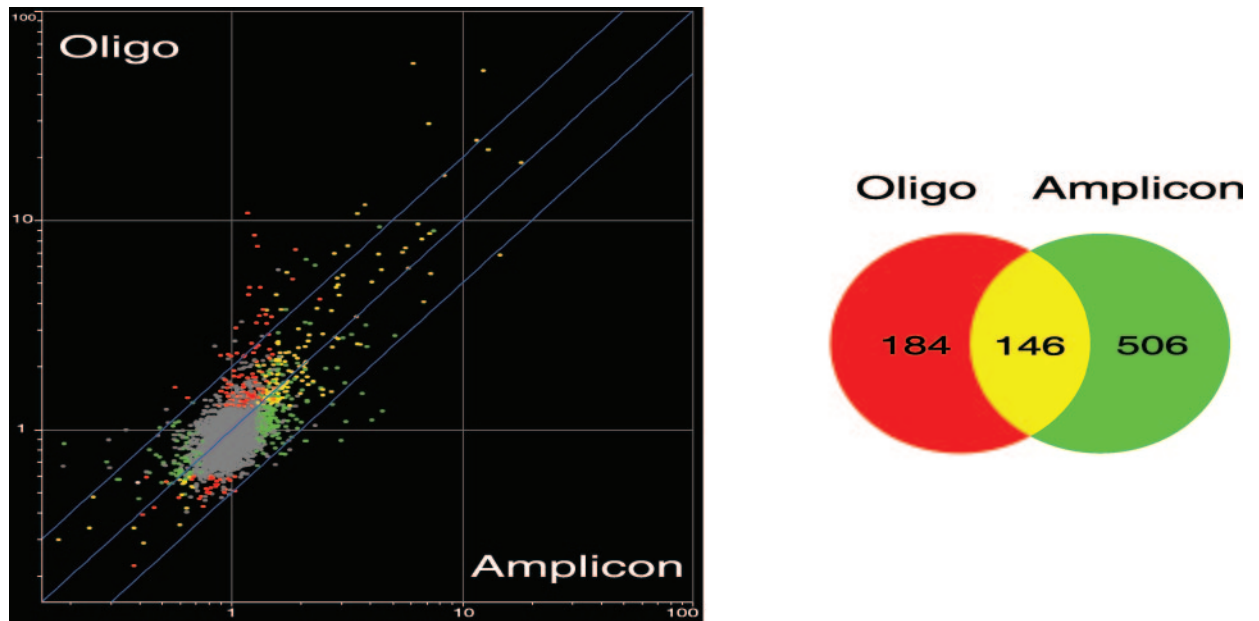


FIG. 11. Similarity between the *myo5* Δ -Y profiles obtained with amplicon and 70-mer oligonucleotide (oligo) DNA microarrays. Shown is a scatter plot of the average fluorescence ratios observed under yeast growth conditions for *myo5* Δ by use of amplicon microarrays versus 70-mer oligonucleotide microarrays. Transcripts with a statistically significant change in abundance (*t* test, $P < 0.05$, coupled to the Benjamini and Hochberg false discovery rate) are colored as indicated in the Venn diagram (red, *myo5* Δ oligonucleotide transcripts; green, *myo5* Δ amplicon transcripts; yellow, overlap). The numbers in the Venn diagram indicate numbers of genes.

Bretscher (45), to result from inadequate recycling of cell wall remodeling proteins, due to defective fluid-phase endocytosis. Similarly, defective fluid-phase endocytosis could result in the absence of polarized lipid rafts at hyphal tips and of raft-associated proteins such as Rvs167p-GFP.

Surprisingly, we found that disruption of the actin cytoskeleton with cytochalasin A or by deleting actin-organizing domains of Myo5p does not trigger a similar transcriptional response. Although transcript levels of some of the stress-induced genes were elevated in the Δ SH3 Δ A mutant, the increase (*n*-fold) in transcript levels was lower. Furthermore, cytochalasin A treatment induced transcript levels for several genes involved in the oxidative stress response and these were not modulated under any other condition, including in our mutants grown in YPD. Thus, specific functions of Myo5p and Sla2p, and not simply generic disturbance of the actin cytoskeleton, are necessary for the observed transcriptional response.

The signal that triggers the modulated gene transcript profile in the *sla2* Δ and *myo5* Δ mutant cells remains unclear. A key membrane or cell wall protein inappropriately localized at the cell surface due to defective endocytosis could be part of a sensing mechanism leading to the response observed. Many of the significantly overexpressed genes in *myo5* Δ and *sla2* Δ are also overexpressed in a strain that lacks the adenylate cyclase Cdc35p (overlap of significant genes in the *myo5* Δ and *cdc35* Δ mutants has a P of $<1e-60$). The *cdc35* Δ mutant displays no apparent cortical actin patch and associated endocytic defect (data not shown), suggesting that a secondary cell wall defect may underlie the particular transcriptional response observed with the *myo5* Δ and *sla2* Δ mutants. Although we did not detect abnormal chitin deposition in the cell wall of the *cdc35* Δ mutant, this strain has been reported to exhibit aberrant cell walls

(Fig. 5) (24). It is known that cell wall defects are sensed by proteins such as Mid2p, Mtl1p, and Wscp1-4 (30), and these proteins may also be involved in sensing and transducing signals to the transcriptional machinery in response to cell wall defects in the *sla2* Δ and *myo5* Δ cortical actin patch mutants.

Contribution of the osmotic stress response and cell wall integrity pathways. We analyzed the contribution of two signaling pathways known to mediate stress responses to the transcriptional changes found in the *sla2* Δ and *myo5* Δ mutant cells. Hog1p is not required for many of the changes in transcript levels observed with the *myo5* Δ or *sla2* Δ mutants. Hog1p was not hyperphosphorylated in mutants as would be expected if the Hog1p pathway were required for the transcript profile observed. As well, very few of the modulated genes showed Hog1p-dependent changes when *HOG1* was deleted in the *myo5* Δ mutant. Finally, the distinct salt sensitivity of the *myo5* Δ and *sla2* Δ mutants compared to that of the *hog1* Δ mutant suggests that a Hog1p-independent signaling pathway is affected and responsible for this sensitivity.

The Slt2p (Mkc1p) MAPK, part of the cell wall integrity signaling pathway, is also not significantly required for the modulation of modified transcript levels observed for the *myo5* Δ mutant. Transcript levels of many genes encoding cell wall, secreted, and stress proteins identified in the *sla2* Δ and *myo5* Δ mutant transcript profiles were also upregulated in *S. cerevisiae* cells challenged with cell wall perturbations that activate the cell wall integrity pathway (9, 20). Because the elevated transcript levels of most of these genes were not dependent on the presence of Mkc1p in the *myo5* Δ mutant, this also indicates that if cell wall defects acted as a signal to promote upregulation of key genes then signaling would not involve activation of the Pkc1p-Mkc1p pathway.

It remains possible that the Hog1p and Mkc1p pathways regulate a redundant set of genes whose expression is unaffected when only one pathway is inactivated. This does not appear to be the case for the *CRH1* and *orf19.5302* genes, whose elevated transcript levels in the *myo5Δ* mutant are dramatically reduced when either *HOG1* or *MKC1* is deleted. Alternatively, a different pathway altogether may control the expression of the genes listed in Table S2 at <http://candida.bri.nrc.ca/papers/myo/>. For example, the calcineurin pathway, which regulates ion homeostasis and is activated by hyperosmotic stress, could be a candidate signaling pathway. A transient increase in Ca^{2+} intracellular levels in response to a hyperosmotic stress activates calcineurin, a Ca^{2+} /calmodulin-dependent type 2B phosphatase (21, 57). This in turn leads to dephosphorylation of transcription factor Crz1p and its relocation to the nucleus (51). Consistent with this hypothesis, we observed that *CRZ1* and *CRZ2* (homologue of *CRZ1*) transcript levels were 5- and 10-fold upregulated, respectively, in the *myo5Δ* mutant. Examination of gene transcript patterns dependent on Crz1 in *S. cerevisiae* exposed to high levels of Ca^{2+} or Na^{+} (59) revealed that the transcript levels of only *CRH1*, *PHO842*, *SAC6*, and *RVS161* appeared to be affected also in the *myo5Δ* and *sla2Δ* mutants, suggesting that this pathway is not significantly involved in mediating the transcript profile observed. Future studies will help uncover the regulatory circuit(s) involved in controlling the genes described in Table S2 at <http://candida.bri.nrc.ca/papers/myo/>.

Although the Hog1p and Mkc1p pathways do not play a major role in the response described herein, we have shown that they are required for the transcript levels of a specific set of genes affected in the *myo5Δ* mutant (see Tables S2 and S4 at <http://candida.bri.nrc.ca/papers/myo/>) as well as a set of genes not affected in the *myo5Δ* mutant (data not shown). The elevated transcript levels observed have also been reported in a similar study (17). Hog1p and Mkc1p may still play an important role in these endocytic mutants, since deletion of *HOG1* or *MKC1* in the *myo5Δ* mutant caused severe growth defects. Synthetic genetic interaction between *HOG1* and *MYO5* or any other genes encoding components of the actin cytoskeleton has not been reported for *S. cerevisiae* or related yeasts. However, the *S. cerevisiae* *mkc1/(slt2)* mutant displays synthetic lethal interactions between mutations in several genes encoding components of the cortical actin cytoskeleton, such as *bni1*, *tpm1*, *rvs161*, and *rvs167* (53).

Avirulence of the myosin I mutant cannot be explained by the altered transcript profile observed. It is believed that virulence of *C. albicans* not only depends on its ability to switch between different morphogenic forms but also requires the coexpression of virulence traits (24, 27, 40). We have shown previously that myosin I, a regulatory component of the actin cytoskeleton, is required for virulence in a systemic infection model system using *Galleria mellonella* or mice (14; data not shown). The avirulent myosin I mutant is unable to form hyphae, and it is possible that this morphogenesis defect accounted for the failure to infect model hosts. Most yeast-to-hypha induced or repressed genes, including *SOD5*, *PHR1*, *PRY4*, *PST1*, *DDR48*, *OPT1*, and *OPT9*, were properly induced or repressed in the *myo5Δ* and *sla2Δ* mutants (see Table S2 at <http://candida.bri.nrc.ca/papers/myo/>), supporting the hypothesis that the ability to generate the hyphal form is required for

virulence. However, the reduced viability of our mutants under stressful conditions is likely to diminish survival in the host and therefore reduce virulence.

ACKNOWLEDGMENTS

We thank Hervé Hogues for designing the 70-mer oligonucleotide microarrays. We are grateful to members of the laboratory, especially Doreen Harcus and Hugo Lavoie, for fruitful discussions.

This work is NRCC publication number 46204, and it was supported by CIHR grant number MOP-42516 and by the National Institute of Dental and Craniofacial Research grant DE144666 to J.B.

REFERENCES

1. Akashi, T., T. Kanbe, and K. Tanaka. 1994. The role of the cytoskeleton in the polarized growth of the germ tube in *Candida albicans*. *Microbiology* **140**:271–280.
2. Alepuz, P. M., E. de Nadal, M. Zapater, G. Ammerer, and F. Posas. 2003. Osmostress-induced transcription by Hot1 depends on a Hog1-mediated recruitment of the RNA Pol II. *EMBO J.* **22**:2433–2442.
3. Alepuz, P. M., A. Jovanovic, V. Reiser, and G. Ammerer. 2001. Stress-induced MAP kinase Hog1 is part of transcription activation complexes. *Mol. Cell* **7**:767–777.
4. Anderson, J. M., and D. R. Soll. 1986. Differences in actin localization during bud and hypha formation in the yeast *Candida albicans*. *J. Gen. Microbiol.* **132**:2035–2047.
5. Asleson, C. M., E. S. Bensen, C. A. Gale, A.-S. Melms, C. Kurischko, and J. Berman. 2001. *Candida albicans* INT1-induced filamentation in *Saccharomyces cerevisiae* depends on Sla2p. *Mol. Cell Biol.* **21**:1272–1284.
6. Audhya, A., and S. D. Emr. 2002. Stt4 PI 4-kinase localizes to the plasma membrane and functions in the Pkc1-mediated MAP kinase cascade. *Dev. Cell* **2**:593–605.
7. Balguería, A., M. Bagnat, M. Bonneau, M. Aigle, and A. M. Breton. 2002. Rvs161p and sphingolipids are required for actin repolarization following salt stress. *Eukaryot. Cell* **1**:1021–1031.
8. Balguería, A., P. Sivadon, M. Bonneau, and M. Aigle. 1999. Rvs167p, the budding yeast homolog of amphiphysin, colocalizes with actin patches. *J. Cell Sci.* **112**:2529–2537.
9. Boorsma, A., H. de Nobel, B. ter Riet, B. Bargmann, S. Brul, K. J. Hellingwerf, and F. M. Klis. 2004. Characterization of the transcriptional response to cell wall stress in *Saccharomyces cerevisiae*. *Yeast* **21**:413–427.
10. Braun, B. R., M. van Het Hoog, C. d'Enfert, M. Martchenko, J. Dungan, A. Kuo, D. O. Inglis, M. A. Uhl, H. Hogues, M. Berriman, M. Lorenz, A. Levitin, U. Oberholzer, C. Bachewich, D. Harcus, A. Marciel, D. Dignard, T. Iouk, R. Zito, L. Frangeul, F. Tekaia, K. Rutherford, E. Wang, C. A. Munro, S. Bates, N. A. Gow, L. L. Hoyer, G. Kohler, J. Morschhauser, G. Newport, S. Znaidi, M. Raymond, B. Turcotte, G. Sherlock, M. Costanzo, J. Ihmels, J. Berman, D. Sanglard, N. Agabian, A. P. Mitchell, A. D. Johnson, M. Whiteway, and A. Nantel. 2005. A human-curated annotation of the *Candida albicans* genome. *PLoS Genet.* **1**:36–57.
11. Bretscher, A. 2003. Polarized growth and organelle segregation in yeast: the tracks, motors, and receptors. *J. Cell Biol.* **160**:811–816.
12. de Nadal, E., L. Casadome, and F. Posas. 2003. Targeting the MEF2-like transcription factor Smp1 by the stress-activated Hog1 mitogen-activated protein kinase. *Mol. Cell Biol.* **23**:229–237.
13. de Nobel, H., C. Ruiz, H. Martin, W. Morris, S. Brul, M. Molina, and F. M. Klis. 2000. Cell wall perturbation in yeast results in dual phosphorylation of the Slit2/Mpk1 MAP kinase and in an Slit2-mediated increase in FKS2-lacZ expression, glucanase resistance and thermotolerance. *Microbiology* **146**:2121–2132.
14. Dunphy, G. B., U. Oberholzer, M. Whiteway, R. J. Zakarian, and I. Boomer. 2003. Virulence of *Candida albicans* mutants toward larval *Galleria mellonella* (Insecta, Lepidoptera, Galleridae). *Can. J. Microbiol.* **49**:514–524.
15. Engqvist-Goldstein, A. E., and D. G. Drubin. 2003. Actin assembly and endocytosis: from yeast to mammals. *Annu. Rev. Cell Dev. Biol.* **19**:287–332.
16. Enjalbert, B., A. Nantel, and M. Whiteway. 2003. Stress-induced gene expression in *Candida albicans*: absence of a general stress response. *Mol. Biol. Cell* **14**:1460–1467.
17. Enjalbert, B., D. A. Smith, M. J. Smith, I. Alam, S. Nicholls, A. J. Brown, and J. Quinn. 2006. Role of the Hog1 stress-activated protein kinase in the global transcriptional response to stress in the fungal pathogen *Candida albicans*. *Mol. Biol. Cell* **17**:1018–1032.
18. Evangelista, M., B. M. Klebl, A. H. Tong, B. A. Webb, T. Leeuw, E. Leberer, M. Whiteway, D. Y. Thomas, and C. Boone. 2000. A role for myosin-I in actin assembly through interactions with Vrp1p, Bee1p, and the Arp2/3 complex. *J. Cell Biol.* **148**:353–362.
19. Fonzi, W. A., and M. Y. Irwin. 1993. Isogenic strain construction and gene mapping in *Candida albicans*. *Genetics* **134**:717–728.
20. Garcia, R., C. Bermejo, C. Grau, R. Perez, J. M. Rodriguez-Pena, J. Francois,

- C. Nombela, and J. Arroyo. 2004. The global transcriptional response to transient cell wall damage in *Saccharomyces cerevisiae* and its regulation by the cell integrity signaling pathway. *J. Biol. Chem.* **279**:15183–15195.
21. Garciadeblas, B., F. Rubio, F. J. Quintero, M. A. Banuelos, R. Haro, and A. Rodriguez-Navarro. 1993. Differential expression of two genes encoding isoforms of the ATPase involved in sodium efflux in *Saccharomyces cerevisiae*. *Mol. Gen. Genet.* **236**:363–368.
 22. Germann, M., E. Swain, L. Bergman, and J. T. Nickels, Jr. 2005. Characterizing the sphingolipid signaling pathway that remedies defects associated with loss of the yeast amphiphysin-like orthologs, Rvs161p and Rvs167p. *J. Biol. Chem.* **280**:4270–4278.
 23. Gualtieri, T., E. Ragni, L. Mizzi, U. Fascio, and L. Popolo. 2004. The cell wall sensor Wsc1p is involved in reorganization of actin cytoskeleton in response to hypo-osmotic shock in *Saccharomyces cerevisiae*. *Yeast* **21**:1107–1120.
 24. Harcus, D., A. Nantel, A. Marcil, T. Rigby, and M. Whiteway. 2004. Transcription profiling of cyclic AMP signaling in *Candida albicans*. *Mol. Biol. Cell* **15**:4490–4499.
 25. Harrison, J. C., E. S. Bardes, Y. Ohya, and D. J. Lew. 2001. A role for the Pkc1p/Mpk1p kinase cascade in the morphogenesis checkpoint. *Nat. Cell Biol.* **3**:417–420.
 26. Ho, J., and A. Bretscher. 2001. Ras regulates the polarity of the yeast actin cytoskeleton through the stress response pathway. *Mol. Biol. Cell* **12**:1541–1555.
 27. Hube, B. 2004. From commensal to pathogen: stage- and tissue-specific gene expression of *Candida albicans*. *Curr. Opin. Microbiol.* **7**:336–341.
 28. Jonsdottir, G. A., and R. Li. 2004. Dynamics of yeast myosin I: evidence for a possible role in scission of endocytic vesicles. *Curr. Biol.* **14**:1604–1609.
 29. Kaksonen, M., Y. Sun, and D. G. Drubin. 2003. A pathway for association of receptors, adaptors, and actin during endocytic internalization. *Cell* **115**:475–487.
 30. Ketela, T., R. Green, and H. Bussey. 1999. *Saccharomyces cerevisiae* Mid2p is a potential cell wall stress sensor and upstream activator of the *PKC1-MPK1* cell integrity pathway. *J. Bacteriol.* **181**:3330–3340.
 31. Kihara, A., and Y. Igarashi. 2002. Identification and characterization of a *Saccharomyces cerevisiae* gene, RSB1, involved in sphingoid long-chain base release. *J. Biol. Chem.* **277**:30048–30054.
 32. Kurischko, C., and R. K. Swoboda. 2000. Cytoskeletal proteins and morphogenesis in *Candida albicans* and *Yarrowia lipolytica*. *Contrib. Microbiol.* **5**:173–184.
 33. Lechler, T., A. Shevchenko, and R. Li. 2000. Direct involvement of yeast type I myosin in Cdc42-dependent actin polymerization. *J. Cell Biol.* **148**:363–373.
 34. Lee, W. L., M. Bezanilla, and T. D. Pollard. 2000. Fission yeast myosin-I, Myo1p, stimulates actin assembly by Arp2/3 complex and shares functions with WASp. *J. Cell Biol.* **151**:789–800.
 35. Martin, H., J. M. Rodriguez-Pachon, C. Ruiz, C. Nombela, and M. Molina. 2000. Regulatory mechanisms for modulation of signaling through the cell integrity Sit2-mediated pathway in *Saccharomyces cerevisiae*. *J. Biol. Chem.* **275**:1511–1519.
 36. Martin, S. W., and J. B. Konopka. 2004. Lipid raft polarization contributes to hyphal growth in *Candida albicans*. *Eukaryot. Cell* **3**:675–684.
 37. Mio, T., M. Adachi-Shimizu, Y. Tachibana, H. Tabuchi, S. B. Inoue, T. Yabe, T. Yamada-Okabe, M. Arisawa, T. Watanabe, and H. Yamada-Okabe. 1997. Cloning of the *Candida albicans* homolog of *Saccharomyces cerevisiae* *GSC1/FKS1* and its involvement in β -1,3-glucan synthesis. *J. Bacteriol.* **179**:4096–4105.
 38. Munro, S. 2003. Lipid rafts: elusive or illusive? *Cell* **115**:377–388.
 39. Nantel, A., D. Dignard, C. Bachewich, D. Harcus, A. Marcil, A. P. Bouin, C. W. Sensen, H. Hogues, M. van het Hoog, P. Gordon, T. Rigby, F. Benoit, D. C. Tessier, D. Y. Thomas, and M. Whiteway. 2002. Transcription profiling of *Candida albicans* cells undergoing the yeast-to-hyphal transition. *Mol. Biol. Cell* **13**:3452–3465.
 40. Nguyen, M. H., S. Cheng, and C. J. Clancy. 2004. Assessment of *Candida albicans* genes expressed during infections as a tool to understand pathogenesis. *Med. Mycol.* **42**:293–304.
 41. Oberholzer, U., A. Marcil, E. Leberer, D. Y. Thomas, and M. Whiteway. 2002. Myosin I is required for hypha formation in *Candida albicans*. *Eukaryot. Cell* **1**:213–228.
 42. Oberholzer, U., T. L. Iouk, D. Y. Thomas, and M. Whiteway. 2004. Functional characterization of myosin I tail regions in *Candida albicans*. *Eukaryot. Cell* **3**:1272–1286.
 43. O'Rourke, S. M., I. Herskowitz, and E. K. O'Shea. 2002. Yeast go the whole HOG for the hyperosmotic response. *Trends Genet.* **18**:405–412.
 44. Pascual-Ahuir, A., F. Posas, R. Serrano, and M. Proft. 2001. Multiple levels of control regulate the yeast cAMP-response element-binding protein repressor Sko1p in response to stress. *J. Biol. Chem.* **276**:37373–37378.
 45. Pruyn, D., and A. Bretscher. 2000. Polarization of cell growth in yeast. *J. Cell Sci.* **113**:571–585.
 46. Pruyn, D., A. Legesse-Miller, L. Gao, Y. Dong, and A. Bretscher. 2004. Mechanisms of polarized growth and organelle segregation in yeast. *Annu. Rev. Cell Dev. Biol.* **20**:559–591.
 47. Roemer, T., B. Jiang, J. Davison, T. Ketela, K. Veillette, A. Breton, F. Tandia, A. Linteau, S. Sillaots, C. Marta, N. Martel, S. Veronneau, S. Lemieux, S. Kauffman, J. Becker, R. Storms, C. Boone, and H. Bussey. 2003. Large-scale essential gene identification in *Candida albicans* and applications to antifungal drug discovery. *Mol. Microbiol.* **50**:167–181.
 48. Samaj, J., F. Baluska, and H. Hirt. 2004. From signal to cell polarity: mitogen-activated protein kinases as sensors and effectors of cytoskeleton dynamics. *J. Exp. Bot.* **55**:189–198.
 49. Sheikh-Hamad, D., and M. C. Gustin. 2004. MAP kinases and the adaptive response to hypertonicity: functional preservation from yeast to mammals. *Am. J. Physiol. Renal Physiol.* **287**:F1102–F1110.
 50. Smith, D. A., S. Nicholls, B. A. Morgan, A. J. Brown, and J. Quinn. 2004. A conserved stress-activated protein kinase regulates a core stress response in the human pathogen *Candida albicans*. *Mol. Biol. Cell* **15**:4179–4190.
 51. Stathopoulos-Gerontides, A., J. J. Guo, and M. S. Cyert. 1999. Yeast calcineurin regulates nuclear localization of the Crz1p transcription factor through dephosphorylation. *Genes Dev.* **13**:798–803.
 52. Tong, A. H., B. Drees, G. Nardelli, G. D. Bader, B. Brannetti, L. Castagnoli, M. Evangelista, S. Ferracuti, B. Nelson, S. Paoluzi, M. Quondam, A. Zucconi, C. W. Hogue, S. Fields, C. Boone, and G. Cesareni. 2002. A combined experimental and computational strategy to define protein interaction networks for peptide recognition modules. *Science* **295**:321–324.
 53. Tong, A. H., G. Lesage, G. D. Bader, H. Ding, H. Xu, X. Xin, J. Young, G. F. Berriz, R. L. Brost, M. Chang, Y. Chen, X. Cheng, G. Chua, H. Friesen, D. S. Goldberg, J. Haynes, C. Humphries, G. He, S. Hussein, L. Ke, N. Krogan, Z. Li, J. N. Levinson, H. Lu, P. Menard, C. Munyana, A. B. Parsons, O. Ryan, R. Tonikian, T. Roberts, A. M. Sdicu, J. Shapiro, B. Sheikh, B. Suter, S. L. Wong, L. V. Zhang, H. Zhu, C. G. Burd, S. Munro, C. Sander, J. Rine, J. Greenblatt, M. Peter, A. Bretscher, G. Bell, F. P. Roth, G. W. Brown, B. Andrews, H. Bussey, and C. Boone. 2004. Global mapping of the yeast genetic interaction network. *Science* **303**:808–813.
 54. Vida, T. A., and S. D. Emr. 1995. A new vital stain for visualizing vacuolar membrane dynamics and endocytosis in yeast. *J. Cell Biol.* **128**:779–792.
 55. Walther, A., and J. Wendland. 2004. Polarized hyphal growth in *Candida albicans* requires the Wiskott-Aldrich syndrome protein homolog Wallp. *Eukaryot. Cell* **3**:471–482.
 56. Wera, S., J. C. Bergsma, and J. M. Thevelein. 2001. Phosphoinositides in yeast: genetically tractable signalling. *FEMS Yeast Res.* **1**:9–13.
 57. Wieland, J., A. M. Nitsche, J. Strayle, H. Steiner, and H. K. Rudolph. 1995. The PMR2 gene cluster encodes functionally distinct isoforms of a putative Na⁺ pump in the yeast plasma membrane. *EMBO J.* **14**:3870–3882.
 58. Woo, M., K. Lee, and K. Song. 2003. MYO2 is not essential for viability, but is required for polarized growth and dimorphic switches in *Candida albicans*. *FEMS Microbiol. Lett.* **218**:195–202.
 59. Yoshimoto, H., K. Saltsman, A. P. Gasch, H. X. Li, N. Ogawa, D. Botstein, P. O. Brown, and M. S. Cyert. 2002. Genome-wide analysis of gene expression regulated by the calcineurin/Crz1p signaling pathway in *Saccharomyces cerevisiae*. *J. Biol. Chem.* **277**:31079–31088.
 60. Yuzyuk, T., and D. C. Amberg. 2003. Actin recovery and bud emergence in osmotically stressed cells requires the conserved actin interacting mitogen-activated protein kinase kinase Ssk2p/MTK1 and the scaffold protein Spa2p. *Mol. Biol. Cell* **14**:3013–3026.
 61. Zhang, X., M. De Micheli, M. Coleman, S. T. Sanglard, and W. S. Moye Rowley. 2000. Analysis of the oxidative stress regulation of the *Candida albicans* transcription factor, Cap1. *Mol. Microbiol.* **36**:618–629.